

Efficient Unit Commitment Constraint Screening under Uncertainty

Xuan He¹, Honglin Wen², Yufan Zhang³, Yize Chen⁴, and Danny H. K. Tsang¹

Abstract—Day-ahead unit commitment (UC) is a fundamental task for power system operators, where generator statuses and power dispatch are determined based on the forecasted nodal net demands. The uncertainty inherent in renewables and load forecasting requires the use of techniques in optimization under uncertainty to find more resilient and reliable UC solutions. However, the solution procedure of such specialized optimization may differ from the deterministic UC. The original constraint screening approach can be unreliable and inefficient for them. Thus, in this work we design a novel screening approach under the forecasting uncertainty. Our approach accommodates such uncertainties in both chance-constrained (CC) and robust forms (RO), and can greatly reduce the UC instance size by screening out non-binding constraints. To further improve the screening efficiency, we utilize the multi-parametric programming (MPP) theory to convert the underlying optimization problem of the screening model to a piecewise affine function. A multi-area screening approach is further developed to handle the computational intractability issues for large-scale problems. We verify the proposed method's performance on a variety of UC setups and uncertainty situations. Experimental results show that our robust screening procedure can guarantee better feasibility, while the CC screening can produce more efficient reduced models. The average screening time for a single line flow constraint can be accelerated by 71.2X to 131.3X using our proposed method.

Index Terms—Unit commitment, uncertainty, optimization

I. INTRODUCTION

Solving the unit commitment (UC) problem in an efficient manner is a fundamental yet challenging task for power system operators [1], [2]. On the one hand, with the proliferation of renewable generation along with demand-side innovations such as electric vehicles (EVs) and smart thermostats, obtaining reliable UC solutions is a nontrivial task under an increasing level of forecasting uncertainties [3]. On the other, UC instances can be NP-hard due to their mixed integer programming (MIP) nature [4], particularly in large-scale systems with numerous transmission constraints, which may render the UC model intractable.

Traditionally in the day-ahead stage, unit commitment using deterministic forecasting has been implemented and worked well for bulk power systems in terms of both solution quality and solution time [5]. Yet with increasing uncertainty, this approach often results in violations of system security constraints during real-time operation, or giving uneconomical decisions due to mismatch between forecasts and realizations. It is thus of operational and economic benefit to *explicitly account for the uncertainty* during operational planning.

Thus both industries and research have been looking into UC under stochastic load and generations [6]. Researchers have resorted to optimization techniques such as chance-constrained optimization [7] and robust optimization [2], [8] to explicitly consider the uncertainty and most of them may be accompanied by specialized recourse policy [9]. Their solution procedure can be different from the deterministic UC but still computationally challenging, while there are limited discussions on acceleration for such a solving process.

In this paper, we address the following research question:

How can we accelerate UC solution process while explicitly considering forecasting uncertainty?

To investigate this question, we resort to finding *reduced problems* for the uncertain UC problems. In particular, our technique is based on the observation that in real-world systems, only a subset of security constraints such as line flow limits are binding or active, while eliminating the non-binding constraints would not change UC problem's solution. Identifying an appropriate subset of line flow limits is known as *constraint screening*. We aim to explore the influence of net demand uncertainty on constraint screening for uncertain UC formulations. In addition, we propose an efficient approach that can not only respect the uncertainty formulation in UC instances, but also greatly accelerate the screening procedure.

Existing work on constraint screening focuses on the deterministic UC formulation. And researchers have developed approaches to conduct screening more efficient or more sufficient [10]–[13]. [10] proposes to solve a screening model maximizing the (bidirectional) line flow for every network constraint for a specific net demand. If the maximal line flow does not reach the line limit, this limit will be identified as redundant. [11], [14] add UC cost bounds to such a screening model to eliminate more constraints. Some recent approaches aim to improve screening efficiency by using machine learning models, such as directly classifying constraint sets [15], [16], predicting total system costs [14], [17], and some warm starting strategies [18], [19].

However, previous screening methods cannot be applied to UC formulations under uncertainty such as robust (RO) [20], [21] and chance-constrained (CC) models [22], [23], as depicted in Fig. I. Robust UC formulation is a computationally viable methodology that provides solutions deterministically immune to any realization of uncertainty within a defined set of uncertainties. CC-UC formulation can better utilize the prior knowledge of the uncertainty distribution, though it may fail in some extreme cases. These uncertain formulations are widely used in UC problems, but so far they have not been sufficiently investigated as to how the prevailing uncertainty would impact the screening results for these formulations. The existing

X. He and D.H.K. Tsang are with the Information Hub, Hong Kong University of Science and Technology (Guangzhou). H. Wen is with Shanghai Jiao Tong University. Y. Zhang is with University of California San Diego. Y. Chen is with University of Alberta, email: yize.chen@ualberta.ca.

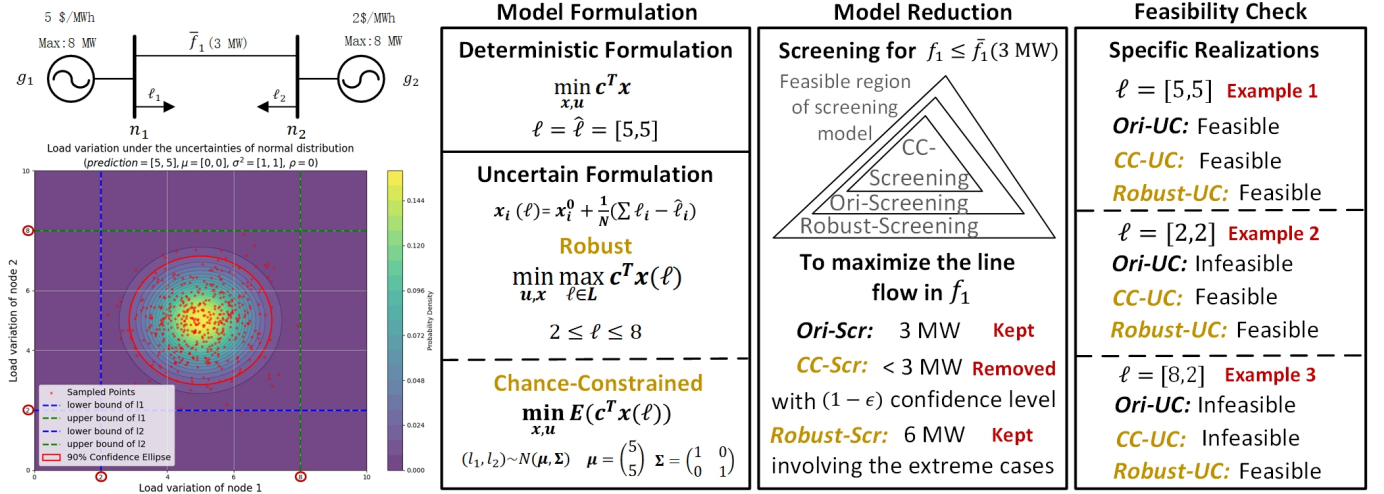


Fig. 1. Our intuition based on a two-node UC problem under net demand uncertainty. The deterministic UC model, based on predicted net demand, may yield infeasible solutions (Example 2-3). The RO-UC model and CC-UC model are developed to obtain solutions that can be reliably adjusted to feasible ones using predefined recourse policies $\mathbf{x}(\ell)$, typically linear decision rules when the exact net demand is known. We propose to conduct constraint screening for different formulations to reduce their complexity. The robust screening can be valid for all formulations and the RO-UC can be feasible under small-probability events (Example 3), while the CC screening may achieve a smaller reduced model equivalent to the original CC-UC model (Example 1-2).

consideration mainly develops different uncertainty sets in the screening model for the deterministic UC model [12], [13], which requires resolving the reduced UC model for the exact realization. The resulting screening results may not be efficient or reliable for the uncertain UC formulations, especially for the CC-UC formulation with a specific distribution and a recourse policy that can directly adjust the initial generation schedule for an exact realization.

By reformulating the screening model for the uncertain UC formulations considering the recourse policies, we can achieve a more suitable screening result. However, there still exists the computation burden arising from solving the optimization problem of the screening model for each line and each net demand instance. [24] proposes to replace the optimization model solving with matrix operations, while in [25], screening time mainly depends on the number of non-redundant constraints rather than the number of lines. Data-driven approaches [15], [16], [26] can also speed up the screening procedure, but there may not be enough historical data for large-scale systems. Besides, these reduced UC models may not be equivalent to the original one [15], [16], [24] or produce a more complicated screening model with considerable binary variables [25]. This motivates us to find more efficient approaches to accelerate the screening procedure with a guarantee of equivalence.

In this work, we show that constraint screening is readily achievable for UC formulations with uncertain net demand involved. More importantly, we show both screening and UC problem-solving can be greatly accelerated using our proposed techniques. The main contributions of our work can be summarized as follows:

- 1) We are the first to conduct constraint screening for the UC formulations under uncertainty. RO-screening and CC-screening models are developed to reduce their original models reliably. The results show that the RO-

screening can achieve 100% feasibility for tested load samples, while the CC-screening can find more redundant constraints.

- 2) A multi-parametric programming (MPP) method is adapted to convert each screening model to a piecewise affine function that maps the input of net demand to the maximal line flow. The results show that the screening procedure can be accelerated by 5.9X to 54.3X compared to directly solving the screening model.
- 3) A decomposition-based multi-area screening is proposed to accelerate the screening procedure reliably for large-scale systems. The results show that the total screening time can be reduced by 6.9%, while the comparable scales and the equivalent solutions can be achieved for the reduced model compared to the cases without decomposition.

II. PRELIMINARIES

A. Deterministic UC model

In the deterministic UC formulation, the system operators need to decide both the ON/OFF statuses (the commitment schedule) \mathbf{u} as well as dispatch level \mathbf{x} for all generators to find the least total costs for time horizon T , corresponding to generators' cost vector \mathbf{c} . Without loss of generality, we denote $x_i(t)$ as the generator i 's generation at timestep t . We follow the typical modeling assumption to model power flows as a DC approximation, where $a_{i,j}$ denotes the entry in the Power Transfer Distribution Factors (PTDF) matrix [27]. \bar{f}_j and \underline{f}_j denote the upper and lower bounds of line flow. We assume that each node has the generation and for the node without generator, we let the corresponding generation bound $\bar{x}_i = 0$. i, j denote the index of the bus and line, respectively. For a deterministic UC instance with N generators involved, the problem can be formulated as

$$\min_{\mathbf{u}, \mathbf{x}} \sum_{t=1}^T \sum_{i=1}^N c_i x_i(t) \quad (1a)$$

$$\text{s.t.} \quad u_i \underline{x}_i \leq x_i(t) \leq u_i \bar{x}_i, \quad \forall i, t, \quad (1b)$$

$$\bar{\mathbf{f}}_j \leq \sum_{i=1}^n a_{i,j} (x_i(t) - \hat{\ell}_i(t)) \leq \bar{\mathbf{f}}_j, \quad \forall j, t, \quad (1c)$$

$$\sum_{i=1}^n x_i(t) - \sum_{i=1}^n \hat{\ell}_i(t) = 0, \quad \forall t, \quad (1d)$$

$$u_i(t) \in \{0, 1\}, \quad \forall i, t, \quad (1e)$$

$$x \in \mathbf{X}_T. \quad (1f)$$

where constraints (1b), (1c) and (1d) denote the generation bound, line flow limits and the system power balance, respectively. (1e) enforces the binary constraint of the generator statuses, where $u_i = 1$ indicates that the generator is on. (1f) denotes the temporal constraint set of generations such as ramping constraints. Note that in the deterministic case, $\hat{\ell}_i(t)$ denotes the net demand considering the load and renewable generation, which is assumed forecasted perfectly and is regarded as the ground truth $\ell_i(t)$, i.e., $\hat{\ell}_i(t) = \ell_i(t)$.

B. Uncertainties from Net Demand and Affine Recourse Policy

However, as mentioned above, operating conditions of the UC problem can be highly influenced by intermittent renewable generation and stochastic load, meaning $\hat{\ell}_i(t) \neq \ell_i(t)$. Thus, the solution obtained by (1) can be infeasible for the ground truth $\ell_i(t)$. To address this issue, UC problems considering variations in net demand of load and renewable generation are developed. For simplification, we only consider the single-step UC problem while the method can be flexibly extended to incorporate the multi-step UC problem. The relationship between the forecast, ground truth, and uncertainty is represented as

$$\hat{\ell} = \ell + \omega. \quad (2)$$

We assume that controllable generators can provide a response $\mathbf{x}(\omega)$ to adapt their generation to the realization of the uncertainty ω . In particular, the response from the generators can ensure that $\mathbf{x}(\omega)$ and the ground-truth ℓ yield a solution that satisfies (1d). We denote the total power mismatch due to prediction errors as $\Omega = \sum_{i=1}^N \omega_i$, which can be distributed among the generators based on participation factors α according to the following generation response policy:

$$x_i(\omega) = x_i + \alpha_i \Omega. \quad (3)$$

where α_i is the participation factor to ensure that a given mismatch is balanced by the same amount of reserve activation, and we have $\sum_{i=1}^N \alpha_i = 1$. Typically, α can be the decision variables to optimize or a specified vector [28]. In this paper we consider the latter case, for the generator participating in balancing the mismatch, we have $\alpha_i = \frac{1}{|G|}$, where $|G|$ denotes the number of the participating controllable generators, and for the others $\alpha_i = 0$.

C. Robust UC Model

Given $\hat{\ell}$, robust formulation includes all possible scenarios of uncertain renewable generation and demand forecasts, and optimizes the UC cost in the worst case, which results in the following min-max formulation:

$$\min_{\mathbf{u}, \mathbf{x}} \max_{\omega} \sum_{i=1}^N c_i x_i(\omega) \quad (4a)$$

$$\text{s.t.} \quad u_i \underline{x}_i \leq x_i(\omega) \leq u_i \bar{x}_i, \quad (4b)$$

$$\bar{\mathbf{f}}_j \leq \sum_{i=1}^N a_{i,j} (x_i(\omega) - \hat{\ell}_i + \omega_i) \leq \bar{\mathbf{f}}_j, \quad (4c)$$

$$\sum_{i=1}^N x_i(\omega) - \sum_{i=1}^N (\hat{\ell}_i - \omega_i) = 0, \quad (4d)$$

$$u_i \in \{0, 1\}. \quad (4e)$$

In this work's robust formulation, we assume that the ground-truth load vector ℓ satisfies the following box uncertainty set, while our method is actually generalizable to a variety of definitions of uncertainty set defined in the domain of robust optimization [2]:

$$\beta_1 \cdot \hat{\ell} \leq \hat{\ell} - \omega \leq \beta_2 \cdot \hat{\ell}. \quad (5)$$

where \cdot denotes the element-wise multiplication, and β_1 and β_2 are scalar vectors associated with each dimension of the forecasted load. Also, note that solving (4) is nontrivial and more time-consuming than solving the original UC problem (1). Thus it is of both research and practical interest to design an acceleration strategy. In the latter sections, we will describe how screening methods can reduce the constraint set of the robust UC formulation, and speed up the robust UC problem solving.

D. Chance-Constrained UC model

Decisions induced by such robust problems can be conservative due to the considerations of worst-case scenarios, thus increasing both the generation reserves and system costs. As such extreme cases are the tails of forecasting distributions, in this paper, a general screening technique also applicable to the chance-constrained formulation of the UC problem is also investigated [29]. CC formulation explicitly limits the probability of constraint violations. Technically, chance constraints depict the maximum allowable violation probability of inequality constraints and reduce the feasible space of the UC problem to a desired confidence region. Mathematically, the

CC-UC problem can be formulated as

$$\min_{\mathbf{u}, \mathbf{x}} \sum_{i=1}^N \mathbb{E}(c_i x_i(\boldsymbol{\omega})) \quad (6a)$$

$$\text{s.t. } \Pr(x_i(\boldsymbol{\omega}) \geq u_i \underline{x}_i) \geq 1 - \epsilon_x, \quad (6b)$$

$$\Pr(x_i(\boldsymbol{\omega}) \leq u_i \bar{x}_i) \geq 1 - \epsilon_x, \quad (6c)$$

$$\Pr(f_j(\boldsymbol{\omega}) \geq -\bar{\mathbf{f}}_j) \geq 1 - \epsilon_f, \quad (6d)$$

$$\Pr(f_j(\boldsymbol{\omega}) \leq \bar{\mathbf{f}}_j) \geq 1 - \epsilon_f, \quad (6e)$$

$$f_j(\boldsymbol{\omega}) = \sum_{i=1}^N a_{i,j}(x_i(\boldsymbol{\omega}) - \hat{\ell}_i + \omega_i), \quad (6f)$$

$$\sum_{i=1}^N x_i(\boldsymbol{\omega}) - \sum_{i=1}^N (\hat{\ell}_i - \omega_i) = 0, \quad (6g)$$

$$u_i \in \{0, 1\}. \quad (6h)$$

The constraints on the controllable generations and line flows are enforced using the separate chance constraints (6b)-(6e). In (6g), the generation response $x_i(\boldsymbol{\omega})$ is selected in a way that maintains the power balance for the possible realization of uncertainty and the response of the system. The chance constraints guarantee that the constraint can satisfy a prescribed probability. The level of risk associated with the chance constraint can be regulated by selecting the probability of violation ϵ_x and ϵ_f [28]. It is noteworthy that for the two formulations considered in this work, the RO-UC model can handle a larger region of uncertainties than the CC-model considering a specific distribution with an acceptable confidence level.

III. CONSTRAINT SCREENING UNDER UNCERTAINTY

As can be seen in Section II, all deterministic and uncertain UC formulations can be large-scale MILP problems that are cumbersome to solve within satisfactory timeframes. Meanwhile, there exist many redundant or inactive constraints as illustrated in Fig. 2, giving the potential to accelerate problem solving of (1), (4) and (6) by screening out such constraints. In this section, we show it is practical to screen out a large number of constraints in these uncertainty-aware UC formulations, which greatly improve solution efficiency for such UC problems.

To identify each redundant line limit under the deterministic case, previous optimization-based screening models [10] evaluate whether line flows $f_j = \sum_{i=1}^n a_{i,j}(x_i - \hat{\ell}_i)$ will hit the limits given the forecasted $\hat{\ell}$:

$$\max_{\mathbf{u}, \mathbf{x}} \text{ or } \min_{\mathbf{u}, \mathbf{x}} f_j \quad (7a)$$

$$\text{s.t. } (1b), (1d), \quad (7b)$$

$$\bar{\mathbf{f}}_k \leq \sum_{i=1}^N a_{i,k}(x_i - \hat{\ell}_i) \leq \bar{\mathbf{f}}_k, \quad k \neq j, \quad (7c)$$

$$0 \leq u_i \leq 1. \quad (7d)$$

where $\hat{\ell}$ is a known net demand vector for UC problem. Note that (7d) relaxes u_i as continuous variables and thus (7) is a tractable linear programming problem.

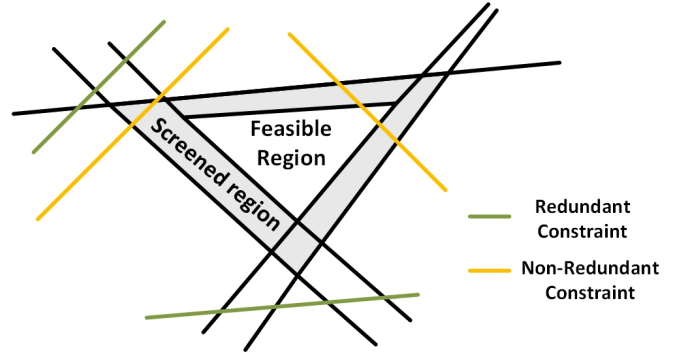


Fig. 2. Redundant constraints identified by the screening models. Feasible regions are defined by all the UC model's constraints, while screened regions are defined by screening model constraints that are part of the UC model.

Inspired by the derivation of the above screening model, in this work we develop the RO-screening and the CC-screening models and we are one of the first to look into such screening problems and to reformulate these models.

A. Robust UC Constraint Screening

According to the optimization-based screening approach, the screening model for the robust UC model can be formulated as follows,

$$\max_{\mathbf{u}, \mathbf{x}, \boldsymbol{\omega}} \text{ or } \min_{\mathbf{u}, \mathbf{x}, \boldsymbol{\omega}} f_j \quad (8a)$$

$$\text{s.t. } (4b), (4d), (5), (3), \quad (8b)$$

$$-\bar{\mathbf{f}}_k \leq \sum_{i=1}^N a_{i,k}(x_i(\boldsymbol{\omega}) - \hat{\ell}_i + \omega_i) \leq \bar{\mathbf{f}}_k, \quad k \neq j, \quad (8c)$$

$$0 \leq u_i \leq 1. \quad (8d)$$

This formulation can identify whether the line flow will hit the limits for all possible realizations satisfying (5) and (3). To further simplify this model and enable the screening results valid for more extreme cases where the recourse policy (3) is absent, the RO-screening model can be relaxed as

$$\max_{\mathbf{u}, \mathbf{x}, \boldsymbol{\omega}} \text{ or } \min_{\mathbf{u}, \mathbf{x}, \boldsymbol{\omega}} f_j \quad (9a)$$

$$\text{s.t. } (4b), (4d), (5), \quad (9b)$$

$$-\bar{\mathbf{f}}_k \leq \sum_{i=1}^N a_{i,k}(x_i - \hat{\ell}_i + \omega_i) \leq \bar{\mathbf{f}}_k, \quad k \neq j, \quad (9c)$$

$$0 \leq u_i \leq 1. \quad (9d)$$

We also have the following Lemma to guarantee the feasibility conditions of the resulting screening model (9):

Lemma 1. Denote the non-redundant line limits of the robust model (4) as $S_{RO-REAL}$, and the non-redundant line limits identified by the screening model (9) as \bar{S}_{RO} . Then $S_{REAL-RO} \subseteq \bar{S}_{RO}$. That is, the constraint screening results obtained by (9) can guarantee the feasibility of (4) unchanged.

Proof. Lemma 1 can be proved by contradiction. Assume that $S_{REAL-RO} \not\subseteq \bar{S}_{RO}$, then this case can occur: for a particular $\hat{\ell} - \tilde{\omega}$, $f_j = \sum_{i=1}^N a_{i,j}(\tilde{x}_i(\tilde{\omega}) - \hat{\ell}_i + \tilde{\omega}_i) = \bar{f}_j$

can hold in (4), while in (9), the obtained maximum of $f_j = \sum_{i=1}^N a_{i,j}(x_i(\tilde{\omega}) - \hat{\ell}_i + \tilde{\omega}_i) < \bar{f}_j$.

However, it can be seen that the feasible solution of (4) will always be feasible for (9). This means in (9) the maximum of $f_j = \sum_{i=1}^N a_{i,j}(x_i(\tilde{\omega}) - \hat{\ell}_i + \tilde{\omega}_i) \geq \sum_{i=1}^N a_{i,j}(\tilde{x}_i(\tilde{\omega}) - \hat{\ell}_i + \tilde{\omega}_i) = \bar{f}_j$. Clearly, $S_{REAL-RO} \subseteq \bar{S}_{RO}$ can be proved by the contradiction. Thus, the screening results given by (9) can guarantee the feasibility of (4) unchanged. \square

Similarly, when (5) is satisfied, it can be proved that the non-redundant line limits of (1) is a subset of \bar{S}_{RO} so that the reduced UC model Testing 3 in Fig. 3 have the same feasibility situation.

B. Chance-Constrained UC Constraint Screening

Unlike the robust model, for the CC-UC model and its screening model, the uncertainty is formulated based on specific random distributions like the Gaussian distribution and the recourse policy is necessary to convert the chance constraints. We need to introduce a new set of optimization variables r_i , which represent the reserve capacity from each generation. Additionally, to guarantee adequate reserves for covering mismatches with high probability, we impose the following chance constraints:

$$\Pr(\alpha_i \Omega \leq r_i) \geq 1 - \epsilon_x, \quad (10a)$$

$$\Pr(\alpha_i \Omega \geq -r_i) \geq 1 - \epsilon_x. \quad (10b)$$

We ensure that scheduled setpoints x_i allow reserves r_i without exceeding generation limits by enforcing:

$$x_i - r_i \geq u_i \underline{x}_i, \quad x_i + r_i \leq u_i \bar{x}_i. \quad (11)$$

Based on the above assumptions, the chance constraints on (6d)-(6e) and (10) with a linear dependence on ω can be exactly reformulated. Previous studies [30], [31] indicated that the normal approximation of renewable generation and load forecasts were plausible in practice. In addition, the use of this assumption is because we are modeling a large number of geographically dispersed wind farms and electricity demands, and the law of large numbers holds [32]. In this work, we thus assume ω follows a Gaussian distribution with mean $\mu_\omega = 0$ and known covariance matrix Σ_ω . The chance-constrained constraint screening model then can be given by:

$$\max_{\mathbf{u}, \mathbf{x}, \mathbf{r}} \text{ or } \min_{\mathbf{u}, \mathbf{x}, \mathbf{r}} f_j(\mathbf{0}) \quad (12a)$$

$$\text{s.t.} \quad u_i \underline{x}_i + r_i \leq x_i \leq u_i \bar{x}_i - r_i, \quad (12b)$$

$$r_i \geq \alpha_i \Phi^{-1}(1 - \epsilon_x) \sigma_\Omega, \quad (12c)$$

$$\mathbb{E}(f_k(\omega)) \geq -\bar{\mathbf{f}}_k + \Phi^{-1}(1 - \epsilon_f) \sigma_{f_k(\omega)}, \quad k \neq j, \quad (12d)$$

$$\mathbb{E}(f_k(\omega)) \leq \bar{\mathbf{f}}_k - \Phi^{-1}(1 - \epsilon_f) \sigma_{f_k(\omega)}, \quad k \neq j, \quad (12e)$$

$$\mathbb{E}(f_k(\omega)) = \sum_{i=1}^N a_{i,k}(x_i - \hat{\ell}_i), \quad (12f)$$

$$\sum_{i=1}^N x_i - \sum_{i=1}^N \hat{\ell}_i = 0, \quad (12g)$$

$$0 \leq u_i \leq 1. \quad (12h)$$

where $\mathbb{E}(f_j(\omega)) = f_j(\mathbf{0})$. σ_Ω and $\sigma_{f_j(\omega)}$ are given as $\sigma_\Omega^2 = \mathbf{1}^T \Sigma_\omega \mathbf{1}$, $\sigma_{f_j(\omega)}^2 = \sum_{i=1}^N a_{i,j}^2 (\sigma_{\omega_i}^2 + \alpha_i^2 \sigma_\Omega^2)$. $\Phi^{-1}(\cdot)$ denotes the inverse Gaussian cumulative distribution, which is used to explicitly transform (10), (6d), (6e) to (12c)-(12e) respectively. The reliability of the chance-constrained screening for the chance-constrained UC model can be guaranteed according to the following analysis:

Lemma 2. Denote the non-redundant line limits of the chance-constrained model (6) as $S_{CC-REAL}$, and the non-redundant line limits identified by the screening model (12) as \bar{S}_{CC} . Then $S_{CC-REAL} \subseteq \bar{S}_{CC}$. The constraint screening results obtained by (12) can guarantee the feasibility of (6) unchanged.

Proof. Lemma 2 can be proved by contradiction. Assume that $S_{CC-REAL} \not\subseteq \bar{S}_{CC}$, then this case can occur: for a particular $\hat{\ell}$, $f_j = \sum_{i=1}^N a_{i,j}(\tilde{x}_i - \hat{\ell}_i) \geq \bar{f}_j$ can hold in (6), while in (12), the obtained maximum of $f_j = \sum_{i=1}^N a_{i,j}(x_i - \hat{\ell}_i) < \bar{f}_j$.

However, due to the fact that the feasible solution of (4) will always be feasible for (9). This means in (12) the maximum of $f_j = \sum_{i=1}^N a_{i,j}(\tilde{x}_i - \hat{\ell}_i) \geq \bar{f}_j$. Then $S_{REAL-CC} \subseteq \bar{S}_{CC}$ can be proved by contradiction. Thus, the screening results given by (12) can guarantee the feasibility of (6) unchanged. \square

Solving the CC-UC screening model (12) will lead to the reduced constraint set \bar{S}_{CC} which will be non-redundant for the original CC-UC problem. Then it is safe to only include such a set for finding CC-UC's solutions.

IV. MPP-BASED SCREENING ACCELERATION

In the real-time operation stage, CC or robust UC models can be applied for the new-coming net demand instance to make the solution resilient to uncertainties. However, in the context of previous screening efforts, solving for each instance can be burdensome, especially for large-scale systems. To address this challenge, we propose the use of a multi-parametric linear programming (MPLP) approach, which is capable of handling varying parameters, such as the forecasted net demand. This approach accelerates the screening process by converting the screening models into affine functions.

A. Mapping Operating Range to Optimal Line Flow

MPLP is a method that enables the objective function and optimization parameters to be expressed as a function of parameters [33]. Indeed, the MPLP method can help find the mapping between the varying parameters of the UC model and the output variables. Our method draws insight from such a procedure, and given any parameter conditions in a predefined set, it is possible to identify the redundant constraints in UC models. Mathematically, consider general linear programming that the parameters appear on the right-hand side of the constraints,

$$\min_{\mathbf{x}} \quad z := \mathbf{a}^T \mathbf{y}, \quad (13a)$$

$$\text{s.t.} \quad \mathbf{A} \mathbf{y} \leq \mathbf{b} + \mathbf{F} \theta, \quad (13b)$$

$$\theta \in \Theta. \quad (13c)$$

where \mathbf{a} , \mathbf{A} , \mathbf{F} , \mathbf{b} are the coefficient vector or matrix with compatible dimensions. θ represents the varying parameters, such

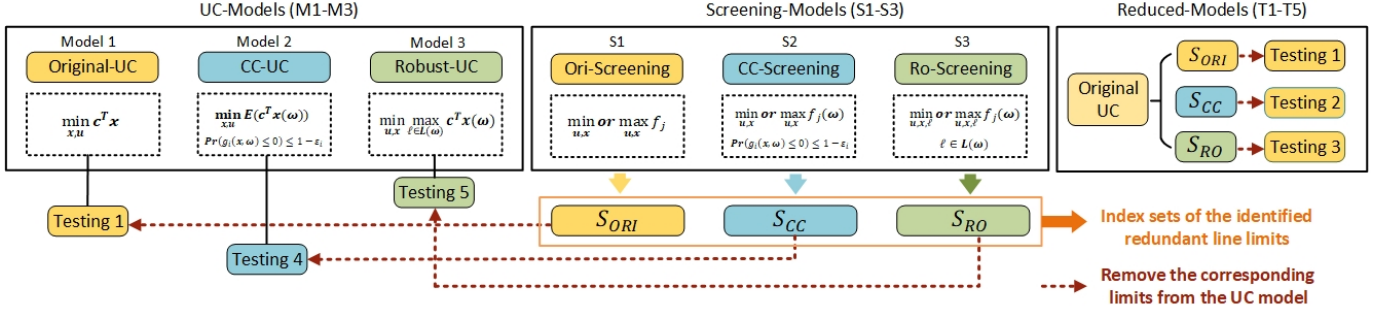


Fig. 3. Relationship among the UC-Models, Screening-Models, and Reduced-Models under different uncertainty settings.

as the nominal load, renewable generation, electricity price, and others. Operators can typically deduce rough operating ranges for these parameters based on historical data. To utilize the MPLP, it is necessary to represent these patterns as a polyhedral convex set denoted by Θ .

Assume that the optimal solution set of (17) is \mathcal{Y}^* , and that each optimal solution $\mathbf{y}^*(\theta) \in \mathcal{Y}^*$ is associated with the parameter θ . By solving the MPLP problem, both critical region $\Theta \subseteq \Theta$ and the parametric expression of $z^*(\theta)$ for Θ (See Fig. 4) can be found. The definition of a critical region is as follows.

Definition 1. Let \mathbf{C} denote the set of constraint indices in (13b), an optimal partition of \mathbf{C} associated with parameter θ is the partition $(\mathbf{C}^A, \mathbf{C}^I)$ where,

$$\mathbf{C}^A(\theta) \triangleq \{j \in \mathbf{C} | \mathbf{A}_j \mathbf{y}^*(\theta) = \mathbf{b}_j + \mathbf{F}_j \theta, \forall \mathbf{y}^*(\theta) \in \mathcal{Y}^*\}, \quad (14a)$$

$$\mathbf{C}^I(\theta) \triangleq \{j \in \mathbf{C} | \mathbf{A}_j \mathbf{y}^*(\theta) < \mathbf{b}_j + \mathbf{F}_j \theta, \exists \mathbf{y}^*(\theta) \in \mathcal{Y}^*\}; \quad (14b)$$

where $\mathbf{A}_j, \mathbf{b}_j, \mathbf{F}_j$ are the j th rows of $\mathbf{A}, \mathbf{b}, \mathbf{F}$. For any $s \subseteq \mathbf{C}$, let \mathbf{A}_s and \mathbf{F}_s be the submatrices of \mathbf{A} and \mathbf{F} , consisting of rows indexed by s . Then the critical region Θ_{s_0} related to $s_0 \subseteq \mathbf{C}$ can be defined as,

$$\Theta_{s_0} \triangleq \{\theta \in \Theta | \mathbf{C}^A(\theta) = s_0\}. \quad (15)$$

which is the set of all parameters $\theta \in \Theta$ with the same active constraints set s_0 at the optimum(s) of problem (17) [34].

Regarding the relationship between the feasible parameter space Θ and critical regions, it can be presented as the following:

Lemma 3. ([35]) Θ can be uniquely partitioned into critical regions $\{\Theta_i\}$ with the assumption that there is no (primal or dual) degeneracy.

Furthermore, the relationship between $z^*(\theta)$ and θ in (17) can be characterized as the following Theorem 1.

Theorem 1. ([35]) The objective function $z^*(\cdot)$ is convex and piecewise affine over Θ (in particular, affine in each critical region θ_i).

To develop the MPLP of the screening models, we consider the forecasted net demand $\hat{\ell}$ as the varying parameter θ , rather than a fixed value in the original screening models (9) and

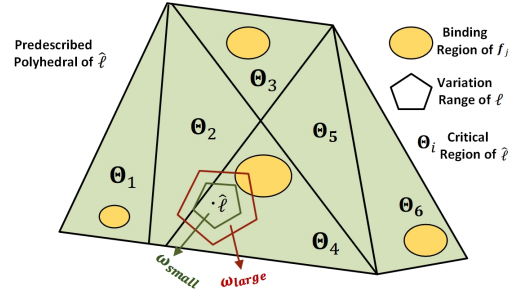


Fig. 4. Critical regions of forecasted net demand $\hat{\ell}$ corresponding to one screening model for line j . In each critical region, there exists an affine function mapping $\hat{\ell}$ to f_j^* . The binding region means that the net demand here can cause maximum line flow to reach the line limit. The uncertainty representation ω can help make the solution more reliable but at the cost of intersecting with more regions Θ .

(12). Using historical data, the operator may have the ability to deduce the variation range of $\hat{\ell}$ for the managed UC instances and represent this range as a polyhedral set $\hat{\Theta}$, as illustrated in Fig. 4. The corresponding MPLP for this setting can be formulated as follows:

$$f_j^*(\mathbf{y}) =: \max_{\mathbf{y}} \text{ or } \min_{\mathbf{y}} f_j \quad (16a)$$

$$\text{s.t. } \mathbf{y} \in \mathcal{Y}(\hat{\ell}), \quad (16b)$$

$$\hat{\ell} \in \hat{\Theta}. \quad (16c)$$

Then, we can deal with the above model via an MPT3 toolbox [36] offline to get the mapping $f_j^*(\hat{\ell})$ between the maximum or minimum of f_j and the incoming forecast of the nominal demand $\hat{\ell}$. In each critical region Θ_i , the mapping is a linear function,

$$f_{i,j}^*(\hat{\ell}) = \hat{\mathbf{a}}_i^T \hat{\ell} + \hat{\mathbf{b}}_i. \quad (17a)$$

where the derivation and computation of critical regions and piecewise affine functions can be found in [33]. Then, the online screening given the specific value of $\hat{\ell}$ can be greatly accelerated by using $f_{i,j}^*(\hat{\ell})$.

B. Decomposition for the Large-Scale System

In practice, large interconnected power systems are typically managed by independent system operators or regional transmission operators. Each operator has its operating area within which internal resources are used economically [37]. Then, the entire system can be decomposed into N_P regions denoted by \mathbf{P} . The original PTDF-based formulation of line

flow relies on all nodes in the entire system, which is hard to be decomposed into subsystems. Therefore, we reformulate the single-step UC into a decomposable model as follows,

$$\min_{\mathbf{u}, \mathbf{x}, \delta} \sum_{g=1}^{N_P} \sum_{i=1}^{N_g} c_i^g x_i^g \quad (18a)$$

$$\text{s.t.} \quad u_i x_i^g \leq x_i^g \leq u_i^g \bar{x}_i^g, \quad i = 1, 2, \dots, N_g, \forall g \in \mathbf{P}, \quad (18b)$$

$$-\bar{\mathbf{f}}_{j,k}^g \leq L_{j,k}^g = \frac{(\delta_j^g - \delta_k^g)}{R_{j,k}} \leq \bar{\mathbf{f}}_{j,k}^g, \quad (j, k) \in \mathbf{F}_g, \forall g \in \mathbf{P}, \quad (18c)$$

$$\sum_{k \in F_{i,k}^g} L_{i,k}^g + x_i^g = \hat{\ell}_i^g, \quad i = 1, 2, \dots, N_g, \forall g \in \mathbf{P}, \quad (18d)$$

$$u_i^g \in \{0, 1\}, \quad i = 1, 2, \dots, N_g, \forall g \in \mathbf{P}, \quad (18e)$$

$$\delta^{ref} = 0. \quad (18f)$$

where N_g is the number of buses in the area g . $R_{j,k}$ is the reactance of the line connecting buses j and k . g is the area index. \mathbf{F}_g is the index set of lines in area g . δ_j^g and δ_k^g are the voltage angles of bus j and bus k , respectively. Note that for a bus i without any unit, x_i^g will be 0. δ^{ref} is the reference bus.

For the whole system, consider the line in the area g connected to the bus w and bus v , the screening model will be

$$\min_{\mathbf{u}, \mathbf{x}, \delta} \text{ or } \max_{\mathbf{u}, \mathbf{x}, \delta} L_{w,v}^g \quad (19a)$$

$$\text{s.t.} \quad (1b), (18d), (18f), \quad (19b)$$

$$-\bar{\mathbf{f}}_{j,k}^g \leq L_{j,k}^g \leq \bar{\mathbf{f}}_{j,k}^g, \quad (j, k) \in \mathbf{F}_{g/(w,v)}, \forall g \in \mathbf{P}, \quad (19c)$$

$$0 \leq u_i^g \leq 1, \quad i = 1, 2, \dots, N_g, \forall g \in \mathbf{P}. \quad (19d)$$

Further, if we only consider the line $(w, v) \in \mathbf{F}_g$ within area g , the screening model will be,

$$\min_{\mathbf{u}, \mathbf{x}, \delta} \text{ or } \max_{\mathbf{u}, \mathbf{x}, \delta} L_{w,v}^g \quad (20a)$$

$$\text{s.t.} \quad u_i x_i^g \leq x_i^g \leq u_i^g \bar{x}_i^g, \quad i = 1, 2, \dots, N_g, \quad (20b)$$

$$-\bar{\mathbf{f}}_{j,k}^g \leq L_{j,k}^g \leq \bar{\mathbf{f}}_{j,k}^g, \quad (j, k) \in \mathbf{F}_{g/(w,v)}, \quad (20c)$$

$$\sum_{k \in F_{i,k}^g} L_{i,k}^g + x_i^g = \hat{\ell}_i^g, \quad i = 1, 2, \dots, N_g, \quad (20d)$$

$$0 \leq u_i^g \leq 1, \quad i = 1, 2, \dots, N_g. \quad (20e)$$

Note that if the reference bus belongs to area g , (18f) will be involved by the screening model (20).

Lemma 4. Denote the non-redundant line limits of the original UC model (18) as S_{ori} , and the non-redundant line limits identified by the whole-screening model (19) as \bar{S}_{whole} and the area-screening model (20) for the area g as \bar{S}_g . Then $S_{ori} \subseteq \bar{S}_{whole} \subseteq \bigcup_{g=1}^{N_P} \bar{S}_g$. The constraint screening results obtained by (20) can guarantee the feasibility of (18) unchanged.

Proof. $S_{ori} \subseteq \bar{S}_{whole}$ has been proved in [10] and thus we only need to prove that $\bar{S}_{whole} \subseteq \bigcup_{g=1}^{N_P} \bar{S}_g$. This can be also proved by contradiction. Assume that $\bar{S}_{whole} \not\subseteq \bigcup_{g=1}^{N_P} \bar{S}_g$, then the following case can occur: for a particular limit of $L_{w,v}^g$, it is identified as a redundant constraint by (20) while it is non-redundant for (19). This means the maximum (or minimum) of (19) is larger (or lower) than that of (20), which indicates that the optimal solution of (19) is not feasible for (20). However, it can be seen that the constraint set of (20) is a subset of the constraint set of (19). This means the feasible solution of (19) will be always feasible for (20). Clearly, $\bar{S}_{whole} \subseteq \bigcup_{g=1}^{N_P} \bar{S}_g$ can be proved by the contradiction and thus $S_{ori} \subseteq \bar{S}_{whole} \subseteq \bigcup_{g=1}^{N_P} \bar{S}_g$ holds. Consequently, the screening results given by (20) can guarantee the feasibility of (18) unchanged. \square

Then, (20) can be solved as an MPLP to get the mapping from the tie-line scheduling to optimal line flow. For the area g , the affine policy set \mathcal{F}_g can be given as,

$$\mathcal{F}_g = \{L_{w,v}^{g,*}(\hat{\ell}_g) = \hat{\mathbf{a}}_i^T \hat{\ell}_g + \hat{\mathbf{b}}_i, i \in \mathbf{I}_{g,j}^\Theta, j \in \mathbf{F}_g\}; \quad (21)$$

where $\mathbf{I}_{g,j}^\Theta$ is the index set of critical region of the line j in area g . For each area $p \in \mathbf{P}$, we can get the affine policy set \mathcal{F}_g and thus achieve the constraint screening for the whole large interconnected power system.

The above multi-area formulations (18) and (20) can be easily extended to the uncertain formulations as (4) and (6), which are still the LPs that can be transferred to the affine policy for acceleration.

V. CASE STUDIES

In this section, we evaluate the performance of the proposed constraint screening method for UC problem under uncertainty and explore the impacts brought by net demand uncertainty upon the screening results over a wide range of problem settings. We demonstrate the clear advantage of the proposed MPP-based screening procedure in both performance and efficiency.

A. Simulation Setup

We carry out the numerical simulations on 39-, 118- and 300-bus power systems to verify the proposed method's effectiveness and scalability. The configurations of the investigated systems are referred to as the corresponding cases in MATPOWER. We select 10 nodes to represent the critical nodes whose load variations are relatively larger and have more impact on the line flows. We assume that there exists the perturbation $\tilde{\omega}$ in the forecasted net demands $\hat{\ell}$ of the selected nodes, and $\hat{\ell}$ is in the predefined polyhedral. To realize different patterns of $\tilde{\omega}$, in the CC-UC cases, we assume $\epsilon_f = \epsilon_x = \epsilon$ and σ_{ω_i} with results given in Table I and Fig. 6-7. In the robust screening cases, we test the settings of β_1 and β_2 given in Table II.

All simulations have been carried out on an unloaded MacBook Air with Apple M1 and 8G RAM. Specifically, all the optimization problems are modeled and solved using YALMIP toolbox and MPT3 toolbox in MATLAB R2022b.

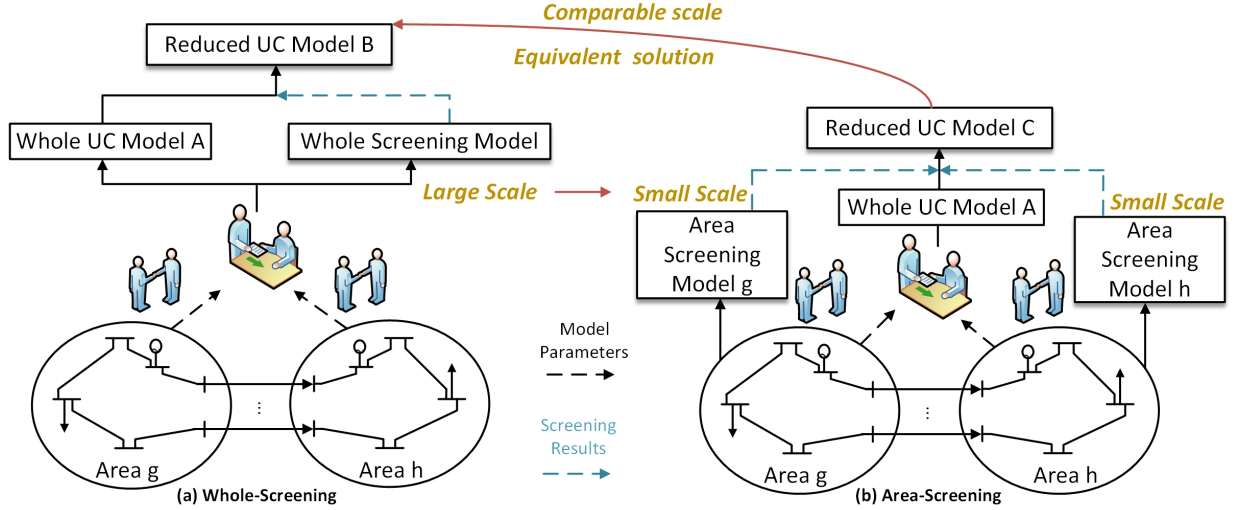


Fig. 5. Schematic of Whole-Screening and Area-Screening approaches. Compared to the whole-screening model, the area-screening models only involves the local variables and constraints, which can be small scale and solved in parallel. Lemma 4 guarantees that the resulted model C is equivalent to model B.

For the sake of convenience, we use the expression given in Fig. 3 to refer to the involved models in the remaining part:

- 1) **UC models:** M1 (Original), M2 (CC) and M3 (Robust).
- 2) **Screening models:** S1 (Original), S2 (CC) and S3 (Robust).
- 3) **Index sets of redundant constraints:** S_{ORI} (given by S1), S_{CC} (given by S2) and S_{RO} (given by S3).
- 4) **Reduced UC models:** T1 (M1 removes S_{ORI}), T2 (M1 removes S_{CC}), T3 (M1 removes S_{RO}), T4 (M2 removes S_{CC}), T5 (M3 removes S_{RO}).

B. Number of Screened Constraints

We solve the screening models S1–S3 for each line limit of 39-bus system and 118-bus system, and record the number of redundant constraints as shown in Fig. 6. It can be seen that S2 tends to find the most redundant constraints, the numbers are 87 and 348. S3 screens out the least, the numbers are 79 and 341. To see this, for the same forecast $\hat{\ell}$, the screened region of S2 is the smallest one and the maximum line flow over this region may not reach the removed line limit in M2. Meanwhile, the corresponding line flow can reach the original line limit in the region outside the screened region of S2. Then, a line limit can be redundant for S2, while it is non-redundant for S1 and S3. On the contrary, the screened region of S3 covers that of S1, so a line limit can be non-redundant for S3, while it is redundant for S1. This corresponds to the fact that robust optimization often considers a more conservative uncertainty set, and in our case, we have more constraints reserved. In Fig. 7, it can be found that even though the line limits and feasible region can be tightened in S2, the locations of the redundant constraints in the topology are still similar to S1 and S3. Besides, most of the lines whose limits are non-redundant are connected or closer to the generators, e.g., line 33-19, line 35-22, and line 38-29, which are expected.

We compare the results of S2 with varying settings of ϵ and σ_{ω_i} in Fig. 6 and Table I. It can be seen that the number of non-redundant limits of the 39-bus system increases to 10 while

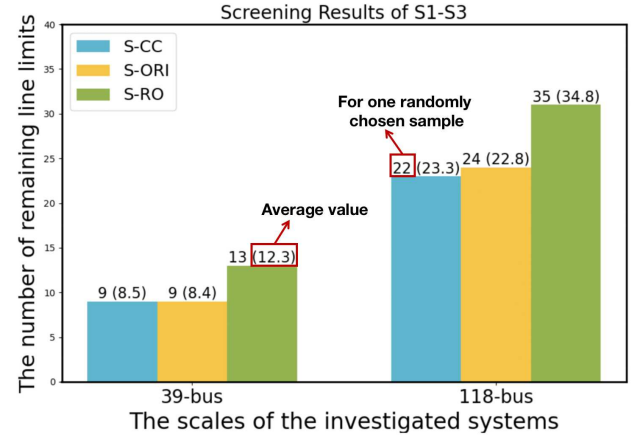


Fig. 6. The number of non-redundant line limits given by original, chance-constrained ($\epsilon = 10\%$, $\sigma_{\omega_i} = 1$) and robust screening ($\beta_1 = 0.7$, $\beta_2 = 1.3$).

TABLE I
FEASIBILITY ANALYSIS OF TESTING 2.

Case	$\epsilon = 5\%, \sigma_{\omega_i} = 1$				$\epsilon = 5\%, \sigma_{\omega_i} = 10$			
	No.Limits	Infea.	Rate	Solu. Gap	No.Limits	Infea.	Rate	Solu. Gap
39	9	0.0%	0.0%		10	10.0%	0.0%	
118	22	0.0%	0.0%		17	5.0%	0.0%	

* 'No. Limits' denotes the number of non-redundant line limits.

that of the 118-bus system decreases to 17 with larger σ_{ω_i} . This indicates that σ_{ω_i} may have a larger impact than ϵ on the binding situations of the constraints in the CC-Screening cases. Regarding the size of S_{RO} , from Table II, it can be found that using S3 will remain more non-redundant constraints for larger variation ranges of uncertainty ω , since there are more binding situations corresponding to the larger load region as shown in Fig. 4.

C. Feasibility of Reduced Problems

After we apply S1–S3 for the forecast $\hat{\ell}$ and remove S_{ORI} , S_{CC} and S_{RO} from M1 respectively offline, we can validate

TABLE II
FEASIBILITY ANALYSIS OF TESTING 3.

Case	$\beta_1(0.9), \beta_2(1.1)$	$\beta_1(0.7), \beta_2(1.3)$	$\beta_1(0.5), \beta_2(1.5)$	Infea. Rate
Bus	No.Limits	No.Limits	No.Limits	
39	10	13	13	0.0%
118	30	35	36	0.0%

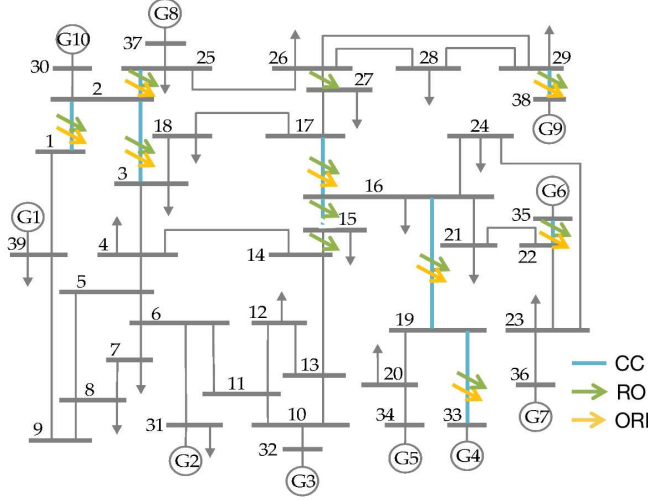


Fig. 7. The identified non-redundant line limits of original, chance-constrained ($\epsilon = 10\%$, $\sigma_{\omega_i} = 10$) and robust ($\beta_1 = 0.7$, $\beta_2 = 1.3$) screening for 39-bus system.

TABLE III
FEASIBILITY ANALYSIS OF TESTING 4.

Case	$\epsilon = 5\%, \sigma_{\omega_i} = 1$				$\epsilon = 5\%, \sigma_{\omega_i} = 10$			
Bus	No.Limits	Infea. Rate	Solu. Gap		No.Limits	Infea. Rate	Solu. Gap	
39	9	3.0%	0.6%		10	7.5%	4.4%	
118	22	0.0%	0.4%		17	5.0%	9.5%	

screening performance of model T1–T3 by obtaining the UC solutions for the groundtruth ℓ . For 39-bus system, S_{ORI} are the same as S_{CC} under the setting of $\epsilon = 5\%$, $\sigma_{\omega_i} = 1$, while under the setting of $\epsilon = 5\%$, $\sigma_{\omega_i} = 10$, the remaining constraints of T2 cover that of T1. As seen from Table I, almost all of the solutions given by T2 are feasible, indicating the solution technique is reliable. The infeasible cases mean the removed constraint will be violated in M1, which can be caused by both T1 and T2.

For T2, it appears that when the deviation caused by uncertainty is small, the solution provided by T2 can achieve a 0% infeasibility rate. On the other hand, when $\sigma_{\omega_i} = 10$, the infeasibility rate increases to 10% for the 39-bus system and 5% for the 118-bus system. For the realizations with feasible solutions, we calculate the gap between the UC costs given by T1 and T2. The results for the 118-bus system suggest that, although the indexes of non-redundant constraints in T2 are a subset of T1, the solution gap might potentially be 0. This observation implies that the actual active line flows for those feasible uncertainty realizations could be a subset of both T1 and T2.

An alternative way to address the impact of uncertainty on the solution of M2 is using the affine generation policy in (3) for T4, allowing direct generation calculation without

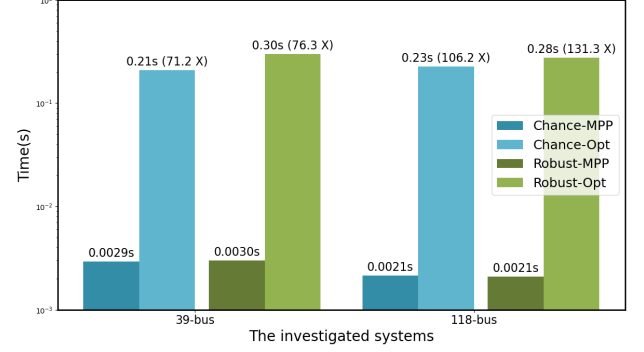


Fig. 8. The average screening time for a single line limit using MPP-based and Optimization-based methods.

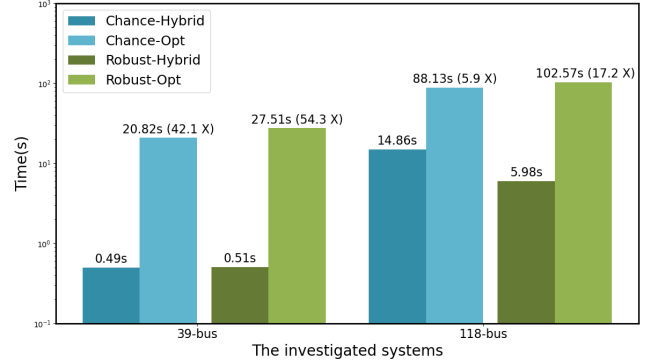


Fig. 9. The total screening times of Hybrid and Optimization only methods.

solving T2 for each uncertainty realization. Results in Table III suggest that infeasibility may arise despite small uncertainty, and for some feasible solutions, like the 118-bus system with $\epsilon = 5\%$, $\sigma_{\omega_i} = 1$, a small gap remains between the actual optimal UC cost and the affine policy-determined cost. As the uncertainty increases, the infeasibility rate might exceed the risk level ϵ , and the solution gap could also become larger. Therefore, although the affine generation policy could potentially reduce the online solution time for the ground truth ℓ , it might also raise the possibility of infeasible solutions.

Regarding the performance of robust screening, Lemma 1 guarantees the feasibility of T5. Besides, the solution provided by T3 will be always feasible for M1 when $\tilde{\omega}$ satisfies (5). Empirical results in Table II support this analysis, as they demonstrate that, for both 39-bus and 118-bus systems, the solutions given by T3 for 200 uncertainty realizations are all feasible for the original UC problem M1, regardless of the three settings for β_1 and β_2 . Note that though T3 offers better feasibility under uncertainty, its solution time is longer than T1 and T2 due to more remaining constraints in the UC model.

TABLE IV
SCREENING RESULTS FOR THE INTERCONNECTED SYSTEM.

Area	Number of binding line limits		$\bar{S}_{whole} \subseteq \bigcup_{g=1}^{N_P} \bar{S}_g?$
	Whole	Decomposed	
39-bus	2045	2068	✓
300-bus	4933	4933	

TABLE V
ONLINE SCREENING TIME OF DIFFERENT METHODS.

Area	Total Time (s)		Time for Single Limit (s)		
	Whole Optimization	Decomposed Optimization	Wh-Opt	De-Opt	De-MPP
39-bus	40203.36	37483.16	17.61	15.42	0.06
300-bus			16.95	16.31	0.13

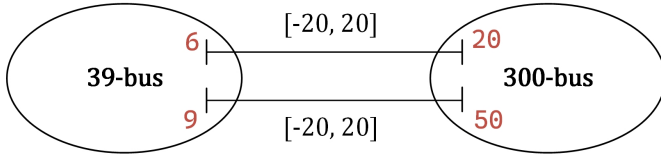


Fig. 10. Interconnected power system consists of 39-bus system and 300-bus system.

D. Screening Time Comparison

To investigate the potential of utilizing MPP to accelerate the screening models with different uncertainty formulations, we develop the affine policy for S2 and S3 via MPP method, respectively. In cases where MPP is not applicable to the screening model or the forecasted load, we revert to solving optimization for S2 and S3 directly, and we can treat this procedure as *hybrid screening*. Consequently, the total screening time of *hybrid screening* is the sum of using affine policy and initial screening. Fig. 8 shows that applying the affine policy can accelerate single-line screening by 71.2X to 131.3X, with more significant improvements in the 118-bus system due to its longer initial screening time compared to the 39-bus system.

Regarding the total screening time, as illustrated in Fig. 9, the screening procedures of 39-bus and 118-bus systems are accelerated by 5.9X to 54.3X via applying the affine policies. The improvements in total screening time are not as substantial as those for single-line screening, potentially because the initial screening time is much longer than the affine policy. Though hybrid screening can add computation time for a few instances, using MPP still reduces the computation burden a lot.

To verify the applicability of decomposed screening, we examine the interconnected power system, comprised of a 39-bus system and a 300-bus system (refer to Fig. 10). We gather the screening results of 100 samples using both whole-screening and area-screening methods, as detailed in Table IV. The number of non-redundant constraints identified by the two screening methods is close, with the results of the whole-screening method being a subset of those obtained from the area-screening method. Regarding the screening time, Table V shows that the decomposed screening can realize 1.1X acceleration for the total time. For a single line limit, the derivation of MPP policy for the whole system fails, while it can work for the decomposed screening model. The online screening procedure can be accelerated from 125X to 257X

via MPP policy for a single line limit of 39-bus or 300-bus system.

VI. CONCLUSION AND FUTURE WORK

In this work, we consider a critical while underexplored constraint screening setting under uncertain electricity demands, along with a novel solution technique for such uncertainty-aware screening problems. The impact of such uncertainty on the screening results, especially the infeasibility of the reduced problems, is investigated both theoretically and empirically under chance-constrained and robust formulations. Further, the multi-parametric program theory and the multi-area screening are demonstrated to be effective for greatly accelerating the screening procedures. This work demonstrates the potential of efficiently and reliably solving UC under forecasting uncertainties. In the future work, it is desirable to assume more general properties of the future load or renewables distribution, which could lead to constraint screening models under distributionally robust settings. We are also interested in investigating the role of data and machine learning for solving UC screening problems.

REFERENCES

- [1] X. Chen, Y. Yang, Y. Liu, and L. Wu, "Feature-driven economic improvement for network-constrained unit commitment: A closed-loop predict-and-optimize framework," *IEEE Transactions on Power Systems*, vol. 37, no. 4, pp. 3104–3118, 2022.
- [2] D. Bertsimas, E. Litvinov, X. A. Sun, J. Zhao, and T. Zheng, "Adaptive robust optimization for the security constrained unit commitment problem," *IEEE transactions on power systems*, vol. 28, no. 1, pp. 52–63, 2012.
- [3] A. J. Conejo, M. Carrión, J. M. Morales *et al.*, *Decision making under uncertainty in electricity markets*. Springer, 2010, vol. 1.
- [4] A. D. Pia, S. S. Dey, and M. Molinaro, "Mixed-integer quadratic programming is in np," *Mathematical Programming*, vol. 162, pp. 225–240, 2017.
- [5] C. Zhao and Y. Guan, "Unified stochastic and robust unit commitment," *IEEE Transactions on Power Systems*, vol. 28, no. 3, pp. 3353–3361, 2013.
- [6] Q. P. Zheng, J. Wang, and A. L. Liu, "Stochastic optimization for unit commitment—a review," *IEEE Transactions on Power Systems*, vol. 30, no. 4, pp. 1913–1924, 2014.
- [7] X. Geng and L. Xie, "Chance-constrained unit commitment via the scenario approach," in *2019 North American Power Symposium (NAPS)*. IEEE, 2019, pp. 1–6.
- [8] S. Zeynali, N. Nasiri, S. N. Ravadanegh, S. Kubler, and Y. Le Traon, "Distributionally robust unit commitment in integrated multi-energy systems with coordinated electric vehicle fleets," *Electric Power Systems Research*, vol. 225, p. 109832, 2023.

- [9] L. A. Roald, D. Pozo, A. Papavasiliou, D. K. Molzahn, J. Kazempour, and A. Conejo, "Power systems optimization under uncertainty: A review of methods and applications," *Electric Power Systems Research*, vol. 214, p. 108725, 2023.
- [10] Q. Zhai, X. Guan, J. Cheng, and H. Wu, "Fast identification of inactive security constraints in scuc problems," *IEEE Transactions on Power Systems*, vol. 25, no. 4, pp. 1946–1954, 2010.
- [11] Á. Porras, S. Pineda, J. M. Morales, and A. Jiménez-Cordero, "Cost-driven screening of network constraints for the unit commitment problem," *arXiv preprint arXiv:2104.05746*, 2021.
- [12] L. A. Roald and D. K. Molzahn, "Implied constraint satisfaction in power system optimization: The impacts of load variations," in *2019 57th Annual Allerton Conference on Communication, Control, and Computing (Allerton)*. IEEE, 2019, pp. 308–315.
- [13] M. Awadalla and F. Bouffard, "Tight and compact data-driven linear relaxations for constraint screening in unit commitment," *IEEE Transactions on Energy Markets, Policy and Regulation*, vol. 2, no. 1, pp. 63–78, 2024.
- [14] X. He, H. Wen, Y. Zhang, and Y. Chen, "Enabling fast unit commitment constraint screening via learning cost model," in *International Conference on Smart Grid Communications (SmartGridComm)*. IEEE, 2024, pp. 1–7.
- [15] S. Zhang, H. Ye, F. Wang, Y. Chen, S. Rose, and Y. Ma, "A data-aided security constraint prescreening technique and application to real-world system," in *2019 North American Power Symposium (NAPS)*. IEEE, 2019, pp. 1–6.
- [16] A. Ardakani and F. Bouffard, "Prediction of umbrella constraints," in *2018 Power Systems Computation Conference (PSCC)*. IEEE, 2018, pp. 1–7.
- [17] S. Pineda, J. M. Morales, and A. Jiménez-Cordero, "Data-driven screening of network constraints for unit commitment," *IEEE Transactions on Power Systems*, vol. 35, no. 5, pp. 3695–3705, 2020.
- [18] Á. S. Xavier, F. Qiu, and S. Ahmed, "Learning to solve large-scale security-constrained unit commitment problems," *INFORMS Journal on Computing*, vol. 33, no. 2, pp. 739–756, 2021.
- [19] A. Jiménez-Cordero, J. M. Morales, and S. Pineda, "Warm-starting constraint generation for mixed-integer optimization: A machine learning approach," *Knowledge-Based Systems*, vol. 253, p. 109570, 2022.
- [20] C. Zhao, J. Wang, J.-P. Watson, and Y. Guan, "Multi-stage robust unit commitment considering wind and demand response uncertainties," *IEEE Transactions on Power Systems*, vol. 28, no. 3, pp. 2708–2717, 2013.
- [21] L. Moretti, E. Martelli, and G. Manzolini, "An efficient robust optimization model for the unit commitment and dispatch of multi-energy systems and microgrids," *Applied Energy*, vol. 261, p. 113859, 2020.
- [22] U. A. Ozturk, M. Mazumdar, and B. A. Norman, "A solution to the stochastic unit commitment problem using chance constrained programming," *IEEE Transactions on Power Systems*, vol. 19, no. 3, pp. 1589–1598, 2004.
- [23] Y. Wang, S. Zhao, Z. Zhou, A. Botterud, Y. Xu, and R. Chen, "Risk adjustable day-ahead unit commitment with wind power based on chance constrained goal programming," *IEEE Transactions on Sustainable Energy*, vol. 8, no. 2, pp. 530–541, 2016.
- [24] Z. Ma, H. Zhong, T. Cheng, J. Pi, and F. Meng, "Redundant and nonbinding transmission constraints identification method combining physical and economic insights of unit commitment," *IEEE Transactions on Power Systems*, vol. 36, no. 4, pp. 3487–3495, 2021.
- [25] A. J. Ardakani and F. Bouffard, "Identification of umbrella constraints in dc-based security-constrained optimal power flow," in *2014 IEEE PES General Meeting — Conference & Exposition*, 2014, pp. 1–1.
- [26] X. He, J. Tian, Y. Zhang, H. Wen, and Y. Chen, "Fast constraint screening for multi-interval unit commitment," in *62nd IEEE Conference on Decision and Control (CDC)*. IEEE, 2023, pp. 577–583.
- [27] Q. Wang, J. D. McCalley, T. Zheng, and E. Litvinov, "A computational strategy to solve preventive risk-based security-constrained opf," *IEEE Transactions on Power Systems*, vol. 28, no. 2, pp. 1666–1675, 2012.
- [28] M. Lubin, Y. Dvorkin, and L. Roald, "Chance constraints for improving the security of ac optimal power flow," *IEEE Transactions on Power Systems*, vol. 34, no. 3, pp. 1908–1917, 2019.
- [29] D. Bienstock, M. Chertkov, and S. Harnett, "Chance-constrained optimal power flow: Risk-aware network control under uncertainty," *Siam Review*, vol. 56, no. 3, pp. 461–495, 2014.
- [30] F. Bouffard and F. D. Galiana, "Stochastic security for operations planning with significant wind power generation," in *2008 IEEE Power and Energy Society General Meeting—Conversion and Delivery of Electrical Energy in the 21st Century*. IEEE, 2008, pp. 1–11.
- [31] B.-M. Hodge, A. Florita, K. Orwig, D. Lew, and M. Milligan, "Comparison of wind power and load forecasting error distributions," National Renewable Energy Lab.(NREL), Golden, CO (United States), Tech. Rep., 2012.
- [32] U. Focken, M. Lange, K. Mönnich, H.-P. Waldl, H. G. Beyer, and A. Luig, "Short-term prediction of the aggregated power output of wind farms—a statistical analysis of the reduction of the prediction error by spatial smoothing effects," *Journal of Wind Engineering and Industrial Aerodynamics*, vol. 90, no. 3, pp. 231–246, 2002.
- [33] N. P. Faísca, V. Dua, and E. N. Pistikopoulos, "Multiparametric linear and quadratic programming," *Multi-Parametric Programming: Volume 1: Theory, Algorithms, and Applications*, vol. 1, pp. 1–23, 2007.
- [34] Y. Ji, R. J. Thomas, and L. Tong, "Probabilistic forecasting of real-time lmp and network congestion," *IEEE Transactions on Power Systems*, vol. 32, no. 2, pp. 831–841, 2016.
- [35] F. Borrelli, A. Bemporad, and M. Morari, "Geometric algorithm for multiparametric linear programming," *Journal of optimization theory and applications*, vol. 118, pp. 515–540, 2003.
- [36] M. Herceg, M. Kvasnica, C. N. Jones, and M. Morari, "Multi-parametric toolbox 3.0," in *2013 European Control Conference (ECC)*, 2013, pp. 502–510.
- [37] Y. Guo, L. Tong, W. Wu, B. Zhang, and H. Sun, "Coordinated multi-area economic dispatch via critical region projection," *IEEE Transactions on Power Systems*, vol. 32, no. 5, pp. 3736–3746, 2017.